

Identification of *Meloidogyne panyuensis* (Nematoda: *Meloidogynidae*) on Orah (*Citrus reticulata* Blanco) and its influence on rhizosphere soil microbial characteristics from Guangxi, China

Xiaoxiao zhang Equal first author, 1, Wei Zhao Equal first author, 1, Yuming Lin 1, Bin Shan 2, Shanshan Yang Corresp. 1

Corresponding Author: Shanshan Yang Email address: yangshanshan12@126.com

Root-knot nematode disease severely affect the yield and quality of the mandarin variety (Citrus reticulata Blanco "Orah") in Guangxi, China. However, the pathogen and the effect of this disease on microbial communities remain poorly understood. This study identified the root-knot nematode *Meloidogyne panyuensis* in the rhizosphere of infected Orah based on morphological and molecular biological methods. Soil chemical properties showed that the organic matter, total nitrogen (TN), total phosphorus (TP), available phosphorus (AP), total potassium (TK), and available potassium (AK) were significantly higher in M. panyuensis-infected Orah rhizosphere soil than in that of healthy plants. The relative abundance of the bacteria Bacillus, Sphingomonas, and Burkholderia-Caballeronia-Paraburkholderia and the fungi Lycoperdon, Fusarium, Neocosmospora, Talaromyces, and Tetragoniomyces was higher in M. panyuensis-infected rhizosphere soil. Furthermore, organic matter, TN, available nitrogen (AN), TP, AP, TK, and AK positively correlated with these bacteria and fungi in M. panyuensis-infected Orah rhizosphere soil. Potential biocontrol strains, such as Burkholderia spp., of root-knot nematode were identified by comparing the differences in rhizosphere microbial composition between healthy Orah and M. panyuensis-infected Orah. Our findings lay a foundation for early warning and prevention of root-knot nematode disease in Orah.

¹ Guangxi Key Laboratory of Agro-Environment and Agric-Products safety, College of Agriculture, Guangxi University, Nanning, China

² Guangxi Subtropical Crops Research Institute, Key Laboratory of Quality and Safety Control for Subtropical Fruit and Vegetable, Ministry of Agriculture and Rural Affairs, Nanning, China



- **Identification of** *Meloidogyne panyuensis*
- 2 (Nematoda: Meloidogynidae) on Orah (Citrus
- 3 reticulata Blanco) and its influence on rhizosphere
- 4 soil microbial characteristics from Guangxi,
- 5 China
- 6 Xiaoxiao Zhang ^{1#}, Wei Zhao ^{1#}, Yuming Lin ¹, Bin Shan ², Shanshan Yang ^{1*}
- 7 Guangxi Key Laboratory of Agro-Environment and Agric-Products safety, College of
- 8 Agriculture, Guangxi University, Nanning, 530004, China
- 9 ² Guangxi Subtropical Crops Research Institute, Key Laboratory of Quality and Safety Control
- 10 for Subtropical Fruit and Vegetable, Ministry of Agriculture and Rural Affairs, Nanning,
- 11 530001, China
- 12 * Corresponding author:
- 13 Shanshan Yang
- 14 No.100, East Daxue Road, Xixiangtang District, Nanning, Guangxi, China
- Email address: yangshanshan12@126.com
- 16 #These authors contributed equally to this study.

17 Abstract

- 18 Root-knot nematode disease severely affect the yield and quality of the mandarin variety (*Citrus*
- 19 reticulata Blanco "Orah") in Guangxi, China. However, the pathogen and the effect of this
- 20 disease on microbial communities remain poorly understood. This study identified the root-knot
- 21 nematode *Meloidogyne panyuensis* in the rhizosphere of infected Orah based on morphological
- 22 and molecular biological methods. Soil chemical properties showed that the organic matter, total
- 23 nitrogen (TN), total phosphorus (TP), available phosphorus (AP), total potassium (TK), and
- 24 available potassium (AK) were significantly higher in *M. panyuensis*-infected Orah rhizosphere
- 25 soil than in that of healthy plants. The relative abundance of the bacteria *Bacillus*,





- 26 Sphingomonas, and Burkholderia-Caballeronia-Paraburkholderia and the fungi Lycoperdon,
- 27 Fusarium, Neocosmospora, Talaromyces, and Tetragoniomyces was higher in M. panyuensis-
- 28 infected rhizosphere soil. Furthermore, organic matter, TN, available nitrogen (AN), TP, AP,
- 29 TK, and AK positively correlated with these bacteria and fungi in *M. panyuensis*-infected Orah
- 30 rhizosphere soil. Potential biocontrol strains, such as *Burkholderia* spp., of root-knot nematode
- were identified by comparing the differences in rhizosphere microbial composition between
- 32 healthy Orah and *M. panyuensis*-infected Orah. Our findings lay a foundation for early warning
- and prevention of root-knot nematode disease in Orah.
- 34 **Keywords:** Citrus reticulata Blanco; Root-knot nematode; Meloidogyne panyuensis;
- 35 Rhizosphere soil; Microbiome



Introduction

38	Citrus was first cultivated in China, where the planting area and yield are far greater than
39	anywhere else. Guangxi Zhuang Autonomous Region has become one of the main citrus-
40	producing areas in China owing to its distinct natural conditions. The planting area of citrus in
41	Guangxi is stable at approximately 53.3×10^5 hectares, and the yield exceeds 11 million ξ
42	annually. Citrus prosuction is the leading industry for local farmers. <u>Increases in market demand</u>
<u>43</u>	and prices have led to the expansion of citrus planting areas in recent years.
44	Citrus reticulata Blanco "Orah" is a hybrid variety, bred by Spiegel-Roy and Vardi (Vardi
45	et al., 2008; Jiang et al., 2011; He et al., 2022) with a high yield, good flavor, and superior
46	quality, which has become the fastest growing late-maturing citrus variety in China (Jiang and
47	Cao, 2011; Qiu et al., 2022). Wuming district of Nanning City (Guangxi Zhuang Autonomous
48	Region) has vigorously developed its Orah industry. In 2022, the planting area of Orah in
49	Wuming reached 30,700 hectares, the yield reached 1.5 million tons, and the annual output value
50	exceeded $$1.4 \times 10^9$. This region is now the largest Orah-producing area in China.
51	The expansion of cultivated areas has increased the occurrence of citrus disease (especially
52	root nematode disease), restricting the yield and quality of citrus. Citrus root-knot nematodes
53	mainly infect new citrus roots and enlarge new root tips or form root knots of varying sizes that
54	cannot elongate normally. Upon infection, the aboveground part of the plant, including the
55	leaves, shortens, the leaves gradually yellow and fall off, and the top twigs wilt. Fourteen types
56	of root-knot nematodes harm citrus, and different regions have different species of root-knot
57	nematodes, such as <i>Meloidogyne incognita</i> and <i>M. javanica</i> in Jiangxi Province (Liao et al.,



1990) and *M. panyuensis* in Sichuan Province (He et al., 2020). Root-knot nematode diseases 58 have rapidly spread with the adjustment of agricultural structure and the development of 59 60 mechanized production, and their occurrence has increased annually. This situation is complex and ever-changing and often involves multiple diseases and nematodes. Identifying pathogenic 61 nematodes and developing targeted prevention and control measures are needed to ensure the 62 63 stable development of the Orah industry. Microorganisms in the soil rhizosphere form symbiotic relationships with the host, and the 64 soil rhizosphere microbiome is important for plant health (Tsang et al., 2020). Abiotic and biotic 65 factors cause dynamic changes in soil rhizosphere microbial communities. Soil chemical 66 properties depend on microbes can influence plant health (Ma et al., 2022). Pseudomonas 67 fluorescens 2-79RN₁₀ protects wheat against take-all disease, and the biocontrol activity of P. 68 fluorescens 2-79RN₁₀ is assisted by the content of Zn and organic matter (Ownley et al., 2003). 69 Moreover, soil chemical properties influence the soil microbial community and cause soil-borne 70 diseases (Li et al., 2022). For example, soil pH and the C to N ratio can affect the microbial 71 community in the rhizosphere soil and further influence plant health (Hogberg et al., 2007; 72 Janvier et al., 2007). *Phellinus noxius* infection affects archaea and fungi in the rhizosphere 73 microbiome (Tsang et al., 2020), and native microbial flora in wilted soil are highly suppressed 74 (Joshi et al., 2021). In addition, the composition of microbial communities in rhizosphere soil 75 can greatly differ between healthy and diseased plants. Healthy watermelons have the lowest 76 abundance of Fusarium oxysporum and pH, and the highest ammonium and nitrate contents 77 (Meng et al., 2019). However, to our knowledge, no studies have focused on the citrus 78



79 rhizosphere microbiome in relation to root-knot nematode infection.

Plant growth promoting rhizobacteria (PGPR) are important components of the plant rhizosphere soil microbial community and are a major biocontrol microbial resource. They can effectively reduce damage to plants caused by environmental stress, maintain the stability of the soil microbial community structure, and significantly antagonize pathogen growth (Zhang et al., 2020). Many independent studies have depicted Proteobacteria as dominant members of the rhizosphere microbiota, such as bacteria from the Pseudomonadaceae or Burkholderiaceae family (Philippot et al., 2013). Root-knot nematodes harm seriously, so it is important to prevent and control root-knot nematode disease, increase yield, reduce environmental pollution and maintain the sustainable development of Orah agriculture.

In this study, the pathogen of Orah root-knot nematode disease was identified in Guangxi.

In this study, the pathogen of Orah root-knot nematode disease was identified in Guangxi.

Likewise, the microbial community and the chemical characteristics of the soil in the rhizosphere of diseased and healthy plants were characterized. This information will help to design integrated management strategies for the disease.

Materials & methods

94 Sample collection

About 6.7 hectares Orah (*Citrus reticulata* Blanco) orchard with a tree age of 3 years under unified agronomic management conditions was investigated in June 2022 in Wuming District,
Nanning City, Guangxi Zhuang Autonomous Region (22°58′45.92″N, 108°11′51.24″E) (Huang et al., 2022). Samples of Orah roots and rhizosphere soil were collected from two adjacent orchards with trees at different stages of growth, one strong and the other short and yellow.



Three rows were randomly selected in healthy or root-knot-infected Orah, and five plants in each row were mixed into one sample. After removing the surface soil, the rhizosphere soil samples were taken. The soil samples were stored in a cooler and transported to the laboratory. The rhizosphere soil was divided into two parts: 1) preserved at -80 °C to determine the rhizosphere soil microbial communities; 2) air-dried to determine soil chemical properties. The healthy Orah samples were marked as CRH, while the root-knot-infected Orah samples were marked as CRN. Egg samples were extracted from the root knots of Orah, purified and inoculated in the roots of disease-susceptible water spinach (Ipomoea aquatica Forsk) in sterilized soil for propagation. Second-stage juveniles (J2s) were collected from hatching eggs. Simultaneously, the fruits of healthy and nematode-infected Orah were collected to evaluate their mass and diameter.

Nematode extraction and identification

Female adults were selected from Orah root-knot tissue under an anatomical microscope, and a slide consisting of 45% lactic acid solution was used to make an impression of the perineal pattern. The tail end of the nematode was cut with a scalpel, and the eggs and other adhesions attached to the inside were carefully removed and slightly modified with a brush, leaving only the perineal pattern part. The perineal pattern was transferred to a glass slide with one drop of pure glycerol, covered with a cover glass, and photographed under an optical microscope (Yang et al., 2021).

One single clean J2s nematode was placed into a 500 μ L centrifuge tube, and 8 μ L ddH2O and 1 μ L 10× PCR buffer was added. The tube was placed in liquid nitrogen for 1 min, then heated to 85°C for 2 min, and this process was repeated 7-8 times. Then, 1 μ L 1 mg/mL



121	proteinase K was added, followed by incubation at 56°C for 1 h and 95°C for 10 min. This
122	nematode genomic DNA was directly used for PCR or stored at -20°C. The rDNA-ITS sequence
123	of the root-knot nematodes was amplified using the universal primers: V5367/26S (5'-
124	TTGATTACGTCCCTGCCCTTT-3'; 5'- TTTCACTCGCCGTTACTAAGG-3') (Vrain, 1993)
125	using the extracted DNA as a template. The obtained rDNA-ITS sequences were compared to
126	other sequences using BLAST (NCBI) and analyzed using the neighbor-joining method with
127	MEGA 6.0 software. The PCR reaction system was performed as followed: 2 μL DNA template,
128	$2~\mu L$ of each primer, $25~\mu L$ of $2\times Rapid$ Taq Master Mix, and $21~\mu L$ ddH2O. The PCR reaction
129	procedure included initial denaturation at 95°C for 3 min, followed by 35 cycles of 95°C for 30 s,
130	55°C for 30 s, and 72°C for 30 s, and a final extension step at 72°C for 5 min, followed by storage
131	at 4°C. The PCR products were examined and sequenced. In addition, specific primers were used
132	to detect nematodes: Mp-F/Mp-R (5'-GTTTTCGGCCCGCAACATGT-3' and 5'-
133	CACCGCCTTGCGTAAACTCC-3'). The PCR reaction system was described above. The PCR
134	reaction procedure included initial denaturation at 95°C for 3 min followed by 30 cycles of 95°C
135	for 30s, 63°C for 30s, 72°C for 45s, and a final extension at 72°C extension 5 min, stored at 4°C.
136	Amplification products were examined by 1% agarose gel electrophoresis for the appearance of a
137	single band as expected 409 bp (He et al., 2020).
138	Healthy Orah seedlings were purchased from the Guangxi Subtropical Crops Research
139	Institute and transplanted into a pot containing sandy loam soil for growth in a greenhouse at
140	room temperature under natural light. After survival, 1000 J2s nematodes were inoculated into
141	the roots of 10 Orah seedlings, another 10 Orah seedlings without nematodes were used as a



negative control. The root soil was removed after three months to observe the damage caused by 142 the nematodes to the roots. 143 Soil chemical properties 144 The chemical properties of soil pH, organic matter, total nitrogen (TN), available nitrogen (AN), 145 total phosphorus (TP), available phosphorus (AP), total potassium (TK), and available potassium 146 147 (AK) were determined as described previously (Bao, 2000). Soil pH was determined using a composite glass electrode meter with a soil: water ratio of 1:2.5. Soil TN was determined using 148 the semi-micro Kjeldahl method, soil AN was determined using a Kjeldahl nitrogen meter, soil 149 150 TP and AP were determined using the molybdenum-antimony anti-colorimetric method, and soil TK and AK were determined using the flame photometric method. 151 **Soil DNA isolation and PCR conditions** 152 153 Total DNA was extracted from each rhizosphere soil sample (0.4 g) using the MoBio PowerSoil kit according to the manufacturer's instructions. The purity and concentration of the extracted 154 DNA were quantified using a Nanodrop spectrophotometer (ND-2000) and on 0.5% agarose 155 156 gels. Bacterial communities were determined using the universal forward primer (338F:5'-ACTCCTACGGGAGGCAGCAG-3') and reverse primer (806R:5'-157 GGACTACHVGGGTWTCTAAT-3') to amplify the 16S rRNA gene (Guo et al., 2019). Fungal 158 communities were examined using the ITS1 gene, amplified using the universal forward primer 159 (ITS1F:5'- CTTGGTCATTTAGAGGAAGTAA-3') and reverse primer (ITS2R:5'-160 GCTGCGTTCTTCATCGATGC-3') (Li et al., 2020). The PCR reaction was performed in a 20 161 μL volume containing 5×FastPfu Buffer 4 μL, 2.5 mM dNTPs 2 μL, each primer 0.8 μL, FastPfu 162



170

171

172

173

174

175

176

177

178

179

180

181

182

183

Polymerase 0.4 μL, bovine serum albumin (BSA) 0.2 μL, soil genomic DNA 10 ng.

Amplifications were performed using an initial denaturation step of 95°C for 3 min, followed by

30 cycles of denaturation at 95°C for 30 s, annealing at 50°C for 30 s, and extension at 72°C for

45 s; with a final extension step at 72°C for 7 min, then stored at 4°C. The PCR products were

purified with a PCR Clean-UpTM kit (MO BioLabs) and sent to the Majorbio Company

(Shanghai, China) for sequencing using an Illumina MiSeq PE300 (Edgar, 2013).

High-throughput sequencing analysis

The raw sequenced sequences were quality-controlled (QC) using fastp software (https://github.com/OpenGene/fastp, version 0.20.0) (Chen et al., 2018), and spliced using FLASH software (http://www.cbcb.umd.edu/software/flash, version 1.2.7) (Magoc and Salzberg, 2011). Quality control involved: filtering bases with quality values below 20 at the end of the reads, setting a window of 50 bp, truncating back-end bases from the window if the average quality value within the window was below 20, filtering reads below 50 bp after QC, and removing reads containing N bases. Pairs of reads were spliced (merged) into one sequence with a minimum overlap length of 10 bp according to the overlap relationship between paired end double-end sequencing reads. The maximum mismatch ratio in the overlap region of the spliced sequence was 0.2, and the non-conforming sequences were screened. The samples were distinguished according to the barcode and primers at the beginning and end of the sequence, and the sequence orientation was adjusted. The number of mismatches of the barcode was 0, and the maximum number of primer mismatches was 2. The data were used for subsequent bioinformatics analyses.



All data analyses were performed using the Meguiar BioCloud platform

(https://cloud.majorbio.com). Alpha diversity Coverage, and Chao 1, Simpson, Shannon, and
Sobs indices were calculated using mothur software (http://www.mothur.org/wiki/Calculators),
and the Wilxocon rank sum test was used to analyze group differences in Alpha diversity and to
complete the dilution curve analysis; the similarity of microbial community structure between
samples was examined using principal coordinate analysis (PCoA) based on the Bray-Curtis
distance algorithm; the analysis of microbial community composition was performed with
python software (https://www.python.org); the Wilxocon rank sum test, two-tailed test, bootstrap
algorithm for microbial community inter-group variation and Bray-Curtis distance algorithm for
correlation with environmental factors were performed using the R-3.3.1 software
(https://www.r-project.org/).

Statistical analysis

- 196 IBM SPSS Statistics 20 was used to analyze <u>significant differences in the growth indicators (the</u>
- 197 fruit mass and diameter of Orah), soil chemical properties, and ecological indicators (Coverage,
- 198 Chao1, Simpson, and Shannon indices).

Results

Rot-knot nematode infection decreased Orah yield

In June, the growth of many Orah infected by root-knot nematode, was weak. Compared with healthy roots, the roots infected by nematodes had root knots of different sizes, and the root disks were together to form fibrous roots, which were messy (Fig 1A, B). The mass and diameter of fruits were significantly lower in rot-knot nematode infected Orah than in healthy Orah (Fig 1C).



The average fruit diameter of healthy Orah was 3.86 cm, which the average fruit diameter of root-knot nematode infected Orah was 2.95 cm, the average fruit diameter of root-knot nematode infected Orah reduced 23.58% than that of healthy Orah (Fig 1D). The average fruit mass of root-knot nematode infected Orah was 7.49 g, which the average fruit mass of healthy Orah was 19.48 g, the average fruit mass of root-knot nematode infected Orah reduced 61.55% than that of healthy Orah (Fig 1E).

Identification of rot-knot nematode infecting Orah

There was slight variation among individuals in the female perineal pattern population, but the degree of variation among populations was similar. Microscopic observation of root-knot nematode populations isolated from Orah showed that the root-knot nematode was *M. panyuensis*: the female was white, spherical to pear-shaped, with obvious neck, and the neck ring was clear. The back ring was not obvious, the excretory orifice was located at the median bulb. The pin was developed, and the basal knob was thick. The perineal pattern was oval, the line was smooth, the back arch was low, and there was no obvious side line (Fig 2A). The morphology of the nematode was consistent with that previously reported. (He et al., 2020).

The length of the obtained rDNA-ITS sequence was 869-870 bp (GenBank accession numbers OR135523-OR135524), Blast results confirmed that those sequences were 97.59-99.08% identical to those of *M. panyuensis* sp. n. from *Arachis hypogaea* L. in Guangdong, China (AY394719.1) (Liao et al., 2005). The phylogenetic tree was constructed based on the rDNA-ITS sequences, and the results showed that *M. panyuensis* from Guangxi was clustered with *M. panyuensis* sp. n. from Guangdong (AY394719.1) (Liao et al., 2005) within a group at a



- value of 100% (Fig 2B). A single 409 bp specific fragment was obtained through PCR
 amplification using the DNA of root-knot nematodes as template and the specific primers Mp-
- 228 F/Mp-R of *M. panyuensis* (Fig 2C).
- Cultured J2s were inoculated into healthy Orah seedlings with good growth, and cultured at room temperature for 3 months. The inoculated roots were found to produce root knots (Fig 2D, E).

232 Soil chemical properties

- 233 Infection with M. panyuensis did not significantly affect the pH but had a great influence on
- organic matter, TN, AN, TP, AP, TK, and AK (Table 1). The organic matter, AP, AK, TN, TP,
- and TK significantly increased in *M. panyuensis*-infected Orah rhizosphere soil by 58.87%,
- 236 14.39%, 521.39%, 37.14%, 52.31%, and 30.34%, respectively compared with those in healthy
- 237 Orah rhizosphere soil.

238

General analyses of the sequencing data

The V3-V4 region of bacterial 16S rDNA and fungal ITS high-throughput sequencing results of
Orah rhizosphere soil samples were analyzed, and 348051 and 382559 optimized sequences were
obtained, respectively. Furthermore, 3509 and 1085 amplicon sequence variant (ASV) sets were
generated using the clustering method. The cluster analysis of the ASVs set covered over 99 %
of the Orah rhizosphere soil microorganisms. This indicated that the sequencing results reflected
the changes in the citrus rhizosphere soil microbial community. The dilution curve of Shannon
and Sobs indices tended to be gentle with increasing sequencing depth (Fig S1). This indicated



251

252

253

254

255

256

257

258

259

260

261

262

263

264

265

266

that the sequencing depth was sufficient to reflect the vast majority of soil bacteria and fungi. In 246 addition, from the ecological index, coverage, it could also reflect that the current sequencing 247 depth was sufficient to cover more than 99 % of soil bacteria and fungi (Table 2). 248 249

Soil bacterial and fungal diversity

The diversity of bacterial and fungal communities in healthy Orah rhizosphere soils was compared with those in M. panyuensis-infected soils. The community richness index (Chao1 index) and community diversity (Shannon index) in M. panyuensis-infected Orah soil increased for bacteria, whereas community diversity (Simpson index) decreased. Meanwhile, the Chaol and Shannon indices in M. panyuensis-infected Orah soil decreased for fungi, whereas the Simpson index increased. However, there was no significant difference between the healthy and M. panyuensis-infected Orah rhizosphere soils (Table 2). The M. panyuensis-infected Orah rhizosphere soil bacterial community was separated from healthy Orah rhizosphere soil bacterial community according to PCoA; the combined horizontal and vertical axes in the figure explained 70.6%; the ANalysis of SIMilarity (ANOSIM) discriminant coefficient R was 0.1852 (Fig 3A). However, the result was not significantly different (P > 0.05). The M. panyuensis-infected Orah rhizosphere soil fungal community partly overlapped with the healthy Orah soil bacterial community. The combined horizontal and vertical axes explained 68.6% of the variance, and the ANOSIM discriminant coefficient R was 0.3704, but the difference was no significant (P > 0.05, Fig 3B). These results showed that there was no significant difference in rhizosphere soil community diversity between healthy and *M. panyuensis*-infected Orah rhizosphere soils.

Soil bacterial and fungal taxonomic composition



267	The <i>M. panyuensis</i> -infected and healthy Orah rhizosphere soils had the same bacterial
268	community composition, and 229 orders were detected. Among them, the relative abundance of
269	Rhizobiales, Burkholderiales, Acidobacteriales, Bacillales, Sphingobacteriales, Bryobacterales,
270	Vicinamibacterales, Frankiales, and Chitinophagales, Ktedonobacterales, Gaiellales, and
271	Xanthomonadales were all above 2%, and were the dominant bacteria in Orah rhizosphere soil.
272	The abundances of the remaining 217 orders were below 2%. The abundance of Burkholderiales
273	in M. panyuensis-infected Orah soil (63%) was significantly higher than the 37% in healthy Orah
274	soil (Fig 4A). In total, 609 genera were identified. Among them, Bacillus, Bryobacter,
275	Sphingomonas, Acidothermus, Burkholderia-Caballeronia-Paraburkholderia, norank-f-n
276	$o-A cidobacteriales, no rank-f-no rank-o-Vicina mibacterales, no rank-f-no rank-o-Gaiella les \ {\tt and}$
277	norank-f-Xanthobacteraceae accounted for over 2%, and were the dominant bacteria in Orah
278	rhizosphere soil. The abundances of the other 600 genera were below 2%. The abundance of
279	Burkholderia-Caballeronia-Paraburkholderia in M. panyuensis-infected Orah soil was 84% (Fig
280	4B). This was significantly higher than the 16% in healthy Orah soil. These results indicate that
281	Burkholderia-Caballeronia-Paraburkholderia were closely related to the occurrence of
282	nematode disease.
283	M. panyuensis-infected and healthy Orah rhizosphere soils had the same fungal community
284	composition, and 11 phyla were detected. Among these, the relative abundances of Ascomycota,
285	Basidiomycota, unclassified_k_Fungi, Rozellomycota, and Mortierellomycota were above 1%,
286	and were the dominant phyla in the rhizosphere soil. The abundances of the other six phyla were
287	below 1%. The abundance of Basidiomycota in M. panyuensis-infected Orah rhizosphere soil



288	was 81%; this was significantly higher than the 19% in healthy Orah rhizosphere soil (Fig 4C). A
289	total of 275 genera were identified. Among these, Lycoperdon, Roussoella, Fusarium,
290	$Neocosmospora, Penicillium, Chaetomium, Talaromyces, Acrocalymma, unclassified_k_Fungi,$
291	and Tetragoniomyces accounted for over 3%, whereas the remaining 265 genera accounted for
292	below 3%. The abundance of Lycoperdon phylum in M. panyuensis-infected Orah rhizosphere
293	soil was 99%; this was significantly higher than the 1% in healthy Orah rhizosphere soil (Fig
294	4D). This indicated that there was a connection between <i>Lycoperdon</i> and the occurrence of
295	nematode disease.
296	Comparative analysis between groups of healthy and M. panyuensis-infected
297	Orah soil microbial communities
298	Comparative analysis of bacteria in Orah rhizosphere soil samples showed that the relative
<u>299</u>	abundance of Burkholderia-Caballeronia-Paraburkholderia in M. panyuensis-infected Orah soil
<u>300</u>	was 4.71%. This was 5.44-fold greater than that in healthy Orah rhizosphere soil groups (0.87%).
301	The relative abundance of <i>Bacillus</i> in <i>M. panyuensis</i> -infected Orah rhizosphere soil was 5.53%;
302	this was 1.40-fold greater than that in healthy Orah rhizosphere soil group (3.96%). The relative
303	abundance of Sphingomonas in M. panyuensis-infected Orah rhizosphere soil was 3.75%; this
304	was 1.50-fold greater than that in healthy Orah rhizosphere soil groups (2.50%) (Fig 5A). These
305	results further indicated a relationship between Burkholderia-Caballeronia-Paraburkholderia,
306	Bacillus, Sphingomonas, and nematode diseases.
307	Comparative analysis of fungi in Orah rhizosphere soil samples showed that the relative
308	abundance of <i>Lycoperdon</i> in <i>M. panyuensis</i> -infected Orah rhizosphere soil was 19.55%; this was



309	77.01-fold greater than that in healthy Orah rhizosphere soil groups (0.2506%). The relative
310	abundance of Fusarium in M. panyuensis-infected Orah rhizosphere soil was 11.06%; this was
311	1.68-fold greater than that in healthy Orah rhizosphere soil groups (6.58%). The relative
312	abundance of <i>Neocosmospora</i> in <i>M. panyuensis</i> -infected Orah soil was 11.22%; this was 2.50-
313	fold greater than that in healthy Orah rhizosphere soil groups (4.48%). The relative abundance of
314	Talaromyces in M. panyuensis-infected Orah rhizosphere soil was 7.98%; this was 12.28-fold
315	greater than that in the healthy Orah soil group (0.65%). The relative abundance of
316	Tetragoniomyces in M. panyuensis-infected Orah rhizosphere soil was 3.79%; this was 189.50-
317	fold greater than that in the healthy Orah rhizosphere soil group (0.02%) (Fig 5B). These results
318	further indicated that there was a relationship between Lycoperdon, Fusarium, Neocosmospora,
319	Talaromyces, Tetragoniomyces, and nematode disease.
320	Correlation analysis between healthy and M. panyuensis-infected Orah soil
321	microbial communities and environmental factors
322	Redundancy analysis (RDA) showed that soil organic matter and available N, P, and K were
323	significantly and positively correlated with the bacterial community in M. panyuensis-infected
324	Orah rhizosphere soil. The explanatory degrees of the horizontal and vertical coordinates were
325	46.02% and 28.01%, respectively. Soil organic matter and available K showed strong correlation
<u>326</u>	coefficients (r2) of 0.9982 and 0.9693, respectively (Fig 6A). Total N, P, and K were
327	significantly positively correlated with the bacterial community in M. panyuensis-infected Orah
328	rhizosphere soil. The interpretations of the horizontal and vertical coordinates were 39.05% and
329	27.83%, respectively. Total N and K showed a strong positive correlation, with correlation

coefficients (r²) of 0.9342 and 0.9055, respectively (Fig 6B). In addition, four of the ten genera 330 with the highest relative abundance were positively correlated with the bacterial community in 331 M. panyuensis infected Orah rhizosphere soil, including Burkholderia-Caballeronia-332 Paraburkholderia (Fig 6A, B). These results add further evidence that Burkholderia-333 Caballeronia-Paraburkholderia were related to nematode infection. 334 335 The soil organic matter and available N, P, and K were significantly positively correlated with the fungal community in M. panyuensis-infected Orah rhizosphere soil. The horizontal and 336 vertical coordinates were 58.18% and 20.09%, respectively. Soil organic matter showed a strong 337 positive correlation with a correlation coefficient (r²) of 0.9116 (Fig 6C). Total N, P, and K were 338 significantly positively correlated with the fungal community in M. panyuensis-infected Orah 339 rhizosphere soil. The interpretations of the horizontal and vertical coordinates were 47.58% and 340 20.74%, respectively. Among these, total P and total K showed strong positive correlations, with 341 correlation coefficients (r²) of 0.9031 and 0.8856, respectively (Fig 6D). In addition, four of the 342 ten genera with the highest relative abundance were positively correlated with the fungal 343 community in the M. panyuensis-infected Orah rhizosphere soil, including Lycoperdon (Fig 6C, 344 D). These results provided further evidence that *Lycoperdon* was related to nematode infection. 345 **Discussion** 346 In recent years, Wuming District of Nanning City, Guangxi Zhuang Autonomous Region has 347 vigorously developed the Orah industry, increased policy support, strengthened scientific and 348 technological support, strictly controlled product quality and safety, vigorously carried out brand 349



creation, and focused on brand effect to drive product marketing. The production base drives
product processing and promotes the development of the whole industrial chain of Orah. In 2022,
Wuming became the largest Orah production area in China, but the disease occurs seriously
during planting, and plant parasitic nematodes were one of the important pathogens on Orah,
which could cause slow and declining production of Orah trees, resulting in a serious decline in
yield and quality. With the adjustment of agricultural structure and the development of
mechanized production, the spread of root knot nematode diseases was rapid, and the occurrence
was increasing year by year. The situation was complex and ever-changing, often involving
multiple diseases and nematodes. The identification of plant nematode pathogens was a
prerequisite and foundation for conducting research on nematode diseases. It was crucial to
quickly and accurately identify pathogenic nematodes and develop targeted prevention and
control measures to ensure the stable development of the Orah industry. This study identified rot-
knot nematode collected from Orah in Wuming. Morphological and molecular biology analyses
revealed that the pathogenic nematode was M. panyuensis. M. panyuensis sp. n. was first isolated
from peanuts in Guangzhou Province (Liao et al., 2005). This nematode was also detected in
guava and pepper in Hainan, and citrus in Hunan (Rui et al., 2005; Wang et al., 2007). This was
the first study showing that <i>M. panyuensis</i> harms Orah in Guangxi Zhuang Autonomous Region.
Rhizosphere microorganisms that constitute the core of plant rhizosphere functions play
important roles in plant growth and development. They are regarded as the second genome of



371	development by increasing the mobility of nutrients in the soil and help plants resist pathogen
372	attacks (Cook et al., 1995; Haney et al., 2015). This study was the first to examine the effects of
373	M. panyuensis on the structure and diversity of bacterial and fungal rhizosphere microbiomes in
374	Orah. A comparison of the rhizosphere soil from root-knot nematode-infected and healthy Orah
375	showed no significant difference in the community diversity of bacteria and fungi. The effect of
376	M. panyuensis infection on rhizosphere microorganisms was mainly manifested in the abundance
377	of microbial populations.
378	The bacterial community in rhizosphere soil plays a key role in suppressing soil-borne plant
379	diseases (Ling et al., 2014; Wang et al., 2017). The bacterial community of Orah infected with
380	M. panyuensis was significantly different from that of healthy Orah and corresponded to
381	increased disease severity. This was consistent with previous reports, for example, the soil
382	bacterial community suppresses plant soil-borne diseases in developing soil upon organic
383	fertilization, and contributes to the control of Fusarium sp. ACCC 36194 (Chen et al., 2020). At
384	the order level, the relative abundances of Vicinamibacterales, Frankiales, and
385	Ktedonobacterales were significantly reduced in M. panyuensis-infected rhizosphere soil,
386	whereas those of Burkholderiales, Bacillales, Sphingomonadales, and Chitinophagales greatly
387	increased. At the genus level, the relative abundances of Acidothermus,
388	$norank_f_norank_o_Acidobacteriales$, $norank_f_norank_o_Vicinamibacterales$,
389	norank_f_norank_o_Gaiellales, and norank_f_Xanthobacteraceae were significantly higher in
390	healthy rhizosphere soil, whereas the relative abundances of Bacillus, Sphingomonas, and
391	Burkholderia-Caballeronia-Paraburkholderia were higher in M. panyuensis-infected



392	rhizosphere soil. <i>Acidothermus</i> is acidophilic, thermophilic, grows at 37–70°C, and between pH
393	3.5-7.0. Thermoacidic bacteria HB4 has high-temperature cellulose decomposition ability and
394	plays an important role in composting (Ma et al., 2009). An increase in hydrolyzed nitrogen
395	content in hickory root soil decreased pH and significantly increased fertility (Ding et al., 2020).
396	Furthermore, norank_f_norank_o_Acidobacteriales belongs to Acidobacteria, a newly identified
397	bacterial group with degradation characteristics. It is widely present in various natural
398	environments, accounting for 5-46% of the soil bacterial population and is second only to
399	Proteobacteria in some plant roots and soil environments. It contains many bacteria that can
400	produce antibiotics, enzymes, organic acids, and so on (Ellis et al., 2003; Sang-Hoon et al.,
401	2008). The increase in Acidothermus and norank f_norank_o_Acidobacteriales might be
402	beneficial for the growth of Orah and may be used as a potential probiotic for root-knot
403	nematode disease in Orah. Bacillus has strong stress resistance and can secrete various hydrolytic
404	enzymes such as lipase, protease, and amylase. This genus can produce sporesthat exhibit
405	resistance to high-temperaturee and UV radiation. It has a wide antibacterial spectrum, fast
406	reproduction, low production cost, high safety, with a wide variety of types, and is widely used
407	in agricultural disease prevention and control (Wang et al., 2021; Kannan et al., 2022). The
408	increase in its relative abundance may be related to its resistance to root-knot nematode disease.
409	Sphingomonas is an abundant microbial resource that can be used to biodegrade
410	organophosphorus compounds and readily degrades pesticides (Nneby et al., 2010; Sharp et al.,
411	2012). The increase in its relative abundance might be related to the degradation of pesticides
412	used to control nematode diseases. Burkholderia is widely distributed in the soil, water, and plant



413	rhizosphere, and is an important biocontrol and growth-promoting bacterium. Extracellular
414	enzymes produced by this genus can dissolve insoluble phosphorus in soil, promote plant
415	growth, and produce a variety of secondary metabolites that inhibit different fungal diseases (El-
416	Banna and Winkelmann, 1998; Parke and Gurian-Sherman, 2001; Wang et al., 2011; Kim et al.,
417	2012; Gong et al., 2019). The increase in Burkholderia might inhibit the growth of pathogens
418	such as M. panyuensis, although this requires further research.
419	The fungal community in the rhizosphere soil plays an important role in the soil ecological
420	environment. In agricultural production, long-term monoculture and continuous cropping can
421	lead to changes in fungal community diversity. The fungal community of Orah infected with M .
422	panyuensis was significantly different from that of healthy Orah and corresponded to the
423	upregulation of disease severity. This was consistent with previous reports, for example, the
424	abundance of soil-borne disease pathogens Fusarium and Guehomyces increased, whereas that of
425	nematocidal fungi (Arthrobotrys) significantly decreased (Li and Liu, 2019). At the phylum
426	level, the relative abundance of Ascomycota in M. panyuensis-infected rhizosphere soil
427	significantly decreased, whereas that of Basidiomycota significantly increased. At the genus
428	level, the relative abundance of Roussoella, Penicillium, Chaetomium, and Acrocalymma was
429	significantly higher in the healthy rhizosphere soil, whereas that of Lycoperdon, Fusarium,
430	Neocosmospora, Talaromyces, and Tetragoniomyces was higher in M. panyuensis-infected
431	rhizosphere soil. Endophytic <i>Penicillium</i> can colonize their ecological niches and protect host
432	plants against multiple stresses; they exhibit many biological functions that can be used in
433	agriculture, biotechnology, and pharmaceuticals (Toghueo and Boyom, 2020). <i>Chaetomium</i> has



434	potential biocontrol ability, and its metabolites contain a variety of chemicals that can improve
435	soil fertility and stimulate plant growth and induce plants to improve the antioxidant capacity of
436	certain tissues to enhance disease resistance (Gao et al., 2006; Fu and Zhang, 2012). The seed
437	dressing and soil application of Chaetomium globosum is as effective at inhibiting Fusarium as
438	cell suspensions and is even better than the fungicidal mixture in promoting crop growth and
439	reducing vascular wilt incidence (Pothiraj et al., 2021). Moreover, Acrocalymma can suppress
440	soil-borne fungal diseases in cucumbers (Huang et al., 2020). The increase in <i>Penicillium</i> ,
441	Chaetomium, and Acrocalymma might be a potential probiotic benefit for the growth of Orah.
442	Fusarium (Simes et al., 2022; Sun et al., 2022) and Neocosmospora (Gai et al., 2011; Sun et al.,
443	2014) are pathogens that cause many diseases. The infestation by root-knot nematodes causes
444	severe diseases due to their association with other microorganisms. These pathobiomes are
445	known as Meloidogyne-based diseases complexes (Wolfgang et al., 2019). The increase in the
446	abundance of $Fusarium$ and $Neocosmospora$ might be closely related to infection by M .
447	panyuensis. Talaromyces is an important biocontrol bacterium that has a hyperparasitic effect on
448	various pathogens, and its chitinase has strong antibacterial activity (Marois et al., 1984; Madi et
449	al., 1997; Xian et al., 2012). In the present study, the increase in <i>Talaromyces</i> abundance may be
450	related to the inhibition of <i>M. panyuensis</i> .
451	Environmental variables are closely related to microbial communities (Li et al., 2023). Soil
452	elements affect the soil microbial composition; in turn, soil microorganisms can change soil
453	chemical properties (Li et al., 2009). The nitrogen, phosphorus, and potassium contents in the
454	soil are directly related to the microbial biomass of the plant rhizosphere. The carbon content of



455	soil, in the form of available carbon, mainly affects the functional activity of microorganisms.
456	Soil available nutrients can cause changes in soil bacterial and archaeal communities, and the
457	high content of soil nitrogen promotes excessive growth of plants to a certain extent. The
458	aboveground part grows too much, the field is closed, resistance is reduced, and the plant is
459	easily infected by pathogens (Philippot et al., 2013; Tian et al., 2016).
460	In this study, the contents of organic matter, TN, AN, TP, AP, TK, and AK in the M.
461	panyuensis-infected Orah rhizosphere soil were all higher than those in healthy rhizosphere soil.
462	This is consistent with a previous report showing that the TN, AN, TP, AP, TK, and AK of
463	Fusarium wilt-infected watermelon rhizosphere soils were higher than those of healthy
464	rhizosphere soils (Meng et al., 2019). As the samples were collected from Orah orchard where
465	fertilization was a common practice, the greater amount of nutrients in the soil of M. panyuensis-
466	infected Orah compared to that of healthy plants may be due to the atrophy of the roots of
467	diseased plants that are not able to take up nutrients from the soil. This can explain the greatest
468	amount of nutrients in the soil of <i>M. panyuensis</i> -infected Orah. Furthermore, organic matter, TN,
469	AN, TP, AP, TK, and AK were positively correlated with the bacterial communities
470	Burkholderia-Caballeronia-Paraburkholderia, Bacillus, and Sphingomonas and negatively
471	correlated with Acidothermus, norank_f_norank_o_Vicinamibacterales,
472	norank_f_Xanthobacteraceae, norank_f_norank_o_Acidobacteriales and
473	norank_f_norank_o_Gaiellales in the M. panyuensis-infected Orah rhizosphere soil. Organic
474	matter, TN, AN, TP, AP, TK, and AK were all positively correlated with the fungal communities
475	Lycoperdon, Fusarium, Neocosmospora, Talaromyces, and Tetragoniomyces, and negatively



correlated with Roussoella, Penicillium, Chaetomium, and Acrocalymma in the M. panyuensis-476 infected Orah rhizosphere soil. These results suggested that the composition of (and changes in) 477 rhizosphere microorganisms might be regulated by plants. A characteristic of nematode 478 infestation is the proliferation of secondary roots caused by the constant death of infested roots. 479 The changes in microbial abundance in the rhizosphere of M. panyuensis-infected Orah can be 480 481 explained by the greater availability of decomposing organic matter provided by the constant death of roots infested by nematodes. Furthermore, infected plants trigger a 'help-seeking' 482 mechanism that actively secretes secondary metabolites to change the soil chemical properties 483 and affect the composition of root flora. The recruited flora also forms a competitive mechanism 484 for better adaptation to the environment, resulting in the enrichment of bacteria of specific 485 species in the rhizosphere of diseased plants. 486

Conclusion

487

488

489

490

491

492

493

<u>494</u>

495

The root-knot nematode causing disease in Orah was identified as *M. panyuensis*. Further analysis of soil chemical properties and the microbiome showed that there were significant differences in organic matter, TN, AN, TP, AP, TK, and microbial community composition between the *M. panyuensis* infected Orah rhizosphere soil and healthy Orah rhizosphere soil, and there was a correlation between them. A variety of potential biocontrol strains were identified to enrich the diversity of microbial biocontrol agents, especially *Burkholderia* spp., a strain of which isolated. These results can guide the screening of biocontrol strains and provide a scientific basis to prevent and treat root-knot nematode diseases.



496	Declara	ation c	of I	ntere	st

The authors declare that they have no conflict of interest.

498 **Data Availability**

- The following information was supplied regarding data availability: Orah rhizosphere soil
- 500 microbiome was PRJNA1010647. Bacterial microbiomes of the healthy Orah rhizosphere soil
- were SRR25907662, SRR25907661 and SRR25907658; Bacterial microbiomes of the root-knot-
- infected Orah rhizosphere soil were SRR25907657, SRR25907656 and SRR25907655; Fungal
- 503 microbiomes of the healthy Orah rhizosphere soil were SRR25907654, SRR25907653 and
- 504 SRR25907652; Fungal microbiomes of the root-knot-infected Orah rhizosphere soil were
- 505 SRR25907651, SRR25907660 and SRR25907659.

506 Supplementary Material

- Figure S1. The rarefaction analysis of all samples. A (Shannon index) and C (Sob index) were
- 508 the bacterial community; B (Shannon index) and D (Sob index) were the bacterial community.
- Table S1. The raw data for the diameter (Fig 1D) and the mass (Fig 1E) of fruits.
- Table S2. The raw data of soil chemical properties of the healthy and M. panyuensis-infected
- 511 Orah rhizosphere soil (Table 1).

512 Figure legends

- Figure 1. Damage symptom of root-knot nematodes on Orah and effects on yield. A, roots
- of healthy Orah. B, roots of root-knot nematodes infected Orah. C, the fruit appearance of the



- healthy Orah (CRH) and the root-knot nematodes infected Orah (CRN). D, the diameter of fruits.
- 516 E, the mass of fruits.
- Figure 2. Identification of rot-knot nematode infecting Orah. A, Perineal pattern of nematode
- female isolated from infected Orah root. Scale bar: 20 μm. B, phylogenetic tree based on rDNA-
- 519 ITS of *Meloidogyne* spp. C, specific amplification using the primers Mp-F/Mp-R in M.
- *panyuensis* isolated from infected Orah. M: DL 2000 Plus; 1-5: negative control (1. Water; 2-3.
- 521 M. incognita; 4-5. M. enterolobii.); 6-13: M. panyuensis. D-E, the disease symptoms on Orah
- 522 caused by M. panyuensis.
- Figure 3. Principal coordinate analysis (PCoA) of bacterial (A) and fungal (B) communities
- based on bray-curtis distances. The circle marked green represented healthy Orah rhizosphere
- soil, and the triangle marked yellow represented *M. panyuensis*-infected Orah rhizosphere soil.
- Figure 4. Relationship between species and samples in rhizosphere soil of healthy and M.
- 527 panyuensis-infected Orah. A (order level) and B (genus level) were the bacterial community; C
- 528 (phylum level) and D (genus level) were the bacterial community.
- 529 Figure 5. Comparative analysis of bacterial (A) and fungal (B) community in rhizosphere
- soil of healthy and *M. panyuensis*-infected Orah. The rectangle on top marked green
- represented healthy Orah rhizosphere soil, and the rectangle below marked red represented M.
- 532 panyuensis-infected Orah rhizosphere soil.
- Figure 6. Redundancy analysis (RDA) between healthy and M. panyuensis-infected Orah



rhizosphere soil microbial communities and environmental factors. A and B were the 534 bacterial community; C and D were the fungal community. The circle marked green represents 535 healthy Orah rhizosphere soil, and the triangle marked yellow represents M. panyuensis-infected 536 Orah rhizosphere soil. 537 538 Table 1. Soil chemical properties of healthy and M. panyuensis-infected Orah rhizosphere 539 soil. 540 Table 2. Richness and diversity estimation of 16S and ITS1 sequencing libraries in healthy 541 and M. panyuensis-infected Orah rhizosphere soil. References 542 543 Bao SD. 2000. Soil and agricultural chemistry analysis. Beijing, China Agriculture Press. 544 Chen D, Wang X, Zhang W, Zhou Z, Ding C, Liao Y, Li X. 2020. Persistent organic fertilization reinforces 545 soil-borne disease suppressiveness of rhizosphere bacterial community. Plant Soil 452(1): 313-328. 546 Chen S, Zhou Y, Chen Y, Gu J. 2018. fastp: an ultra-fast all-in-one FASTQ preprocessor. Bioinformatics 547 34(17): i884-i890. 548 Cook RJ, Thomashow LS, Weller DM, Fujimoto D, Mazzola M, Bangera G, Kim DS. 1995. Molecular 549 mechanisms of defense by rhizobacteria against root disease. Proceedings of the National Academy of Sciences 550 of the United States of America 92(10): 4197-201. 551 Ding LZ, Jin J, Wang ZY, Zhou JM, Tong ZP, Zhou PS, Ma SS. 2020. Changes of soil fertility in carya 552 cathayensis stands in major production towns of Lin'an City (in Chinese with English abstract). Journal 553 *Zhejiang for science technology* 40(03): 45-50. 554 Edgar RC. 2013. UPARSE: highly accurate OTU sequences from microbial amplicon reads. Nature Methods 555 10(10): 996-8. 556 El-Banna N and Winkelmann G. 1998. Pyrrolnitrin from Burkholderia cepacia: antibiotic activity against

fungi and novel activities against streptomycetes. Journal of Applied Microbiology 85(1): 69-78.

557



- 558 Ellis RJ, Morgan P, Weightman AJ, Fry JC. 2003. Cultivation-dependent and -independent approaches for
- 559 determining bacterial diversity in heavy-metal-contaminated soil. Applied and Environmental Microbiology
- 560 69(6): 3223-3230.
- 561 Fu W and Zhang XY. 2012. Progress in antimicrobial mechanism of chaetomium. Chinese Agricultural
- 562 Science Bulletin 28(07): 100-103.
- Gai Y, Pan R, Xu D, Ji C, Deng M, Chen W. 2011. First report of soybean *Neocosmospora* stem rot caused by
- Neocosmospora vasinfecta var. vasinfecta in China. Plant Disease 95(8): 1031-1031.
- 565 Gao KX, Pang YD, Qin NH, Liu XG, Kang ZS. 2006. Synergistic antifungal activity of antibiotics and
- 566 hydrolytic enzymes from endophytic Chaetomium spirale ND35. Acta Phytopathologica Sinica 36(4), 347-
- 567 358.
- 568 Gong AD, Zhu ZY, Lu YN, Wan HY, Wu NN, Cheelo D, Gong S, Wen ST, Hou X. 2019. Functional analysis
- 569 of Burkholderia pyrrocinia WY6-5 on phosphate solubilizing, antifungal and growth-promoting activity of
- 570 Maize. Scientia Agricultura Sinica 52(09): 1574-1586.
- 571 Guo D, Fan Z, Lu S, Ma Y, Nie X, Tong F, Peng X. 2019. Changes in rhizosphere bacterial communities
- during remediation of heavy metal-accumulating plants around the Xikuangshan mine in southern China.
- 573 *Scientific Reports* 9(1): 1947.
- Haney CH, Samuel BS, Bush J, Ausubel FM. 2015. Associations with rhizosphere bacteria can confer an
- adaptive advantage to plants. *Nature plants* 15051.
- 576 Huang QH, Liu JM, Hu CX, Wang NN, Zhang L, Mo XF, Li GG, Liao HH, Huang HM, Ji SF, Chen DK.
- 577 2022. Integrative analyses of transcriptome and carotenoids profiling revealed molecular insight into variations
- 578 in fruits color of Citrus reticulata Blanco induced by transplantation. Genomics 114(2): 110291.
- 579 He Q, Wang D, Zhang D, Liu Y, Cheng F. 2020. Identification and PCR detection of citrus root-knot
- 580 nematode in Hunan Province (in Chinese with English abstract). Plant Protection 46(01):179-184.
- 581 He YZ, Li WG, Zhu PP, Wang M, Qiu JY, Sun HQ, Zhang RZ, Liu P, Ling LL, Fu XZ, Chun CP, Cao L, Peng
- LZ. 2022. Comparison between the vegetative and fruit characteristics of 'orah' (*Citrus reticulata* blanco)
- 583 mandarin under different climatic conditions. *Scientia horticulturae* 300: 111064.
- Hogberg MN, Hogberg P, Myrold DD. 2007. Is microbial community composition in boreal forest soils
- determined by pH, C-to-N ratio, the trees, or all three? *Oecologia* 150(4): 590-601.
- Huang L, Niu Y, Su L, Deng H, Lyu H. 2020. The potential of endophytic fungi isolated from cucurbit plants



- 587 for biocontrol of soilborne fungal diseases of cucumber. *Microbiology Research* 231: 126369.
- Janvier C, Villeneuve F, Alabouvette C, Edel-Hermann V, Mateille T, Steinberg C. 2007. Soil health through
- 589 soil disease suppression: Which strategy from descriptors to indicators? Soil Biology and Biochemistry 39(1):
- 590 1-23.
- 591 Jiang D and Cao L. 2011. Introduction performance of late-maturing high-sugar hybrid citrus Orah in
- 592 Chongqing (in Chinese with English abstract). *South China Fruits* 40(05): 33-34.
- 593 Joshi S, Jaggi V, Gangola S, Singh A, Sah VK, Sahgal M. 2021. Contrasting rhizosphere bacterial
- 594 communities of healthy and wilted Dalbergia sissoo Roxb. forests. *Rhizosphere* 17: 100295.
- Kannan C, Divya M, Rekha G, Barbadikar KM, Maruthi P, Hajira SK, Sundaram RM. 2022. Whole genome
- 596 sequencing data of native isolates of *Bacillus* and *Trichoderma* having potential biocontrol and plant growth
- 597 promotion activities in rice ScienceDirect. *Data in Brief* 41:107923.
- 598 Kim S, Lowman S, Hou G, Nowak J, Flinn B, Mei C. 2012. Growth promotion and colonization of
- 599 switchgrass (*Panicum virgatum*) cv. *Alamo* by bacterial endophyte *Burkholderia phytofirmans* strain PsJN.
- 600 Biotechnol Biofuels 5(1): 37.
- 601 Li D, Zhao B, Olk DC, Zhang J. 2020. Soil texture and straw type modulate the chemical structure of residues
- 602 during four-year decomposition by regulating bacterial and fungal communities. Applied Soil Ecology 155:
- 603 103664.
- 604 Li HN, Liu WX, Da L, Wan FH, Cao YY. 2009. Invasive impacts of Ageratina adenophora (Asteraceae) on
- 605 the changes of microbial community structure, enzyme activity and fertility in soil ecosystem. Scientia
- 606 Agricultura Sinica 42(11): 3964-3971.
- 607 Li J, Li S, Huang X, Tang R, Zhang R, Li C, Xu C, Su J. 2022. Plant diversity and soil properties regulate the
- 608 microbial community of monsoon evergreen broad-leaved forest under different intensities of woodland use.
- 609 Science of The Total Environment 821: 153565.
- 610 LI W, CHEN P, WANG Y, LIU Q. 2023. Characterization of the microbial community response to replant
- diseases in peach orchards. *Journal of Integrative Agriculture* 22(4): 1082-1092.
- 612 Li WH and Liu QZ. 2019. Changes in fungal community and diversity in strawberry rhizosphere soil after 12
- years in the greenhouse. *Journal of Integrative Agriculture* 3: 11.
- 614 Liao JL, Yang WC, Feng ZX, Karssen G. 2005. Description of *Meloidogyne panyuensis* sp. n. (Nematoda:
- 615 Meloidogynidae), parasitic on peanut (Arachis hypogaea L.) in China. Russian Journal of Nematology 2: 13.



- 616 Liao Y, Chen X, Deng S. 1990. Preliminary study on citrus root-knot nematode disease (in Chinese with
- English abstract). Acta Agriculturae Universitatis Jiangxi Ensis 2: 5-9.
- Ling N, Deng K, Song Y, Wu Y, Zhao J, Raza W, Huang Q, Shen Q. 2014. Variation of rhizosphere bacterial
- community in watermelon continuous mono-cropping soil by long-term application of a novel bioorganic
- 620 fertilizer. Microbiology Research 169(7-8): 570-578.
- Ma H, Xie C, Zheng S, Li P, Cheema HN, Gong J, Xiang Z, Liu J, Qin J. 2022. Potato tillage method is
- associated with soil microbial communities, soil chemical properties, and potato yield. *Journal of*
- 623 *Microbiology* 60(2): 156-166.
- 624 Ma HL, Gong ZJ, Chen H, Guo WX. 2009. Isolation, screening and identification of high-temperature
- 625 cellulolytic microbes (in Chinese with English abstract). Journal of Anhui Agricultural Science 29(37): 13987-
- 626 13988.
- 627 Madi L, Katan T, Katan J, Henis Y. 1997. Biological control of Sclerotium rolfsii and Verticillium dahliae by
- 628 Talaromyces flavus is mediated by different mechanisms. Phytopathology 87(10): 1054-1060.
- 629 Magoc T and Salzberg SL. 2011. FLASH: fast length adjustment of short reads to improve genome
- assemblies. *Bioinformatics* 27(21): 2957-63.
- Marois JJ, Fravel DR, Papavizas GC. 1984. Ability of *Talaromyces flavus* to occupy the rhizosphere and its
- 632 interaction with Verticillium dahliae. Soil Biology & Biochemistry 16(4): 387-390.
- 633 Meng T, Wang Q, Abbasi P, Ma Y. 2019. Deciphering differences in the chemical and microbial
- 634 characteristics of healthy and Fusarium wilt-infected watermelon rhizosphere soils. Applied Microbiology and
- 635 Biotechnology 103(3): 1497-1509.
- Nneby K, Jonsson A, Stenstrm J. 2010. A new concept for reduction of diffuse contamination by simultaneous
- 637 application of pesticide and pesticide-degrading microorganisms. *Biodegradation* 21(1): 21.
- 638 Ownley BH, Duffy BK, Weller DM. 2003. Identification and manipulation of soil properties to improve the
- 639 biological control performance of phenazine-producing Pseudomonas fluorescens. Applied and Environmental
- 640 *Microbiology* 6(69): 3333-3343.
- 641 Parke JL and Gurian-Sherman D. 2001. Diversity of the *Burkholderia cepacia* complex and implications for
- risk assessment of biological control strains. *Annual Review of Phytopathology* 39: 225-58.
- 643 Philippot L, Raaijmakers JM, Lemanceau P, Van D. 2013. Going back to the roots: the microbial ecology of
- the rhizosphere. *Nature Reviews Microbiology* 11(11): 789-799.



- 645 Pothiraj G, Hussain Z, Singh AK, Solanke AU, Aggarwal R, Ramesh R, Shanmugam V. 2021.
- 646 Characterization of Fusarium Spp. inciting vascular wilt of tomato and its management by a chaetomium-
- based biocontrol consortium. Frontiers in Plant Science 12: 2544.
- 648 Qiu F, Pan Z, Li L, Xia L, Huang G. 2022. Transcriptome analysis of Orah leaves in response to citrus canker
- 649 infection (in Chinese with English abstract). Journal of Fruit Science 39(04): 631-643.
- Rui K, Chen MC, Guo AP, Xiao TB, Xie SH, Wu FL, Liao JL. 2005. The identification of guava root-knot
- 651 nematodes in Hainan province (in Chinese with English abstract). Journal of South China Agricultural
- 652 *University* 04: 53-58.
- Sang-Hoon, Lee, Jong-Ok, Ka, Jae-Chang, Cho. Members of the phylum *Acidobacteria* are dominant and
- 654 metabolically active in rhizosphere soil. FEMS MICROBIOL LETT 2008;285(2): 263-269.
- 655 Sharp RE, Schultz-Jensen N, Aamand J, Srensen SR. Growth characterization and immobilization studies of
- 656 the MCPA pesticide degrader strain *Sphingomonas* sp. Erg5. 2012 Symposium of The Danish Microbiological
- 657 Society. Nov 2012. Copenhagen, Denmark. 2012.
- 658 Simes D, Diogo E, Andrade ED. 2022. First Report of *Fusarium andiyazi* presence in portuguese Maize
- 659 kernels. *Agriculture* 12(3): 1-5.
- Sun Q, Xie YJ, Chen TM, Zhang JP, Laborda P, Wang SY. 2022. First report of Fusarium avenaceum causing
- canker disease on Kiwi tree in China. *Plant Disease* 6: 106.
- 662 Sun SL, Kim MY, Van K, Lee YH, Zhong C, Zhu ZD, Lestari P, Lee YW, Lee SH. 2014. First report of
- 663 Neocosmospora vasinfecta var. vasinfecta causing soybean stem rot in south Korea. Plant Disease 10(3): 231-
- 664 235.
- 665 Tian Q, Yang X, Wang X, Liao C, Li Q, Wang M, Wu Y, Liu F. 2016. Microbial community mediated
- 666 response of organic carbon mineralization to labile carbon and nitrogen addition in topsoil and subsoil.
- 667 *Biogeochemistry* 128(1-2): 125-139.
- Toghueo RMK and Boyom FF. 2020. Endophytic penicillium species and their agricultural, biotechnological,
- and pharmaceutical applications. 3 BIOTECH 10(3): 107.
- Tsang KSW, Cheung MK, Lam RYC, Kwan HS. 2020. A preliminary examination of the bacterial, archaeal,
- and fungal rhizosphere microbiome in healthy and *Phellinus noxius*-infected trees. *Microbiologyopen* 9(10):
- 672 e1115.
- 673 Vardi A, Levin I, Carmi N. 2008. Induction of seedlessness in citrus: from classical techniques to emerging

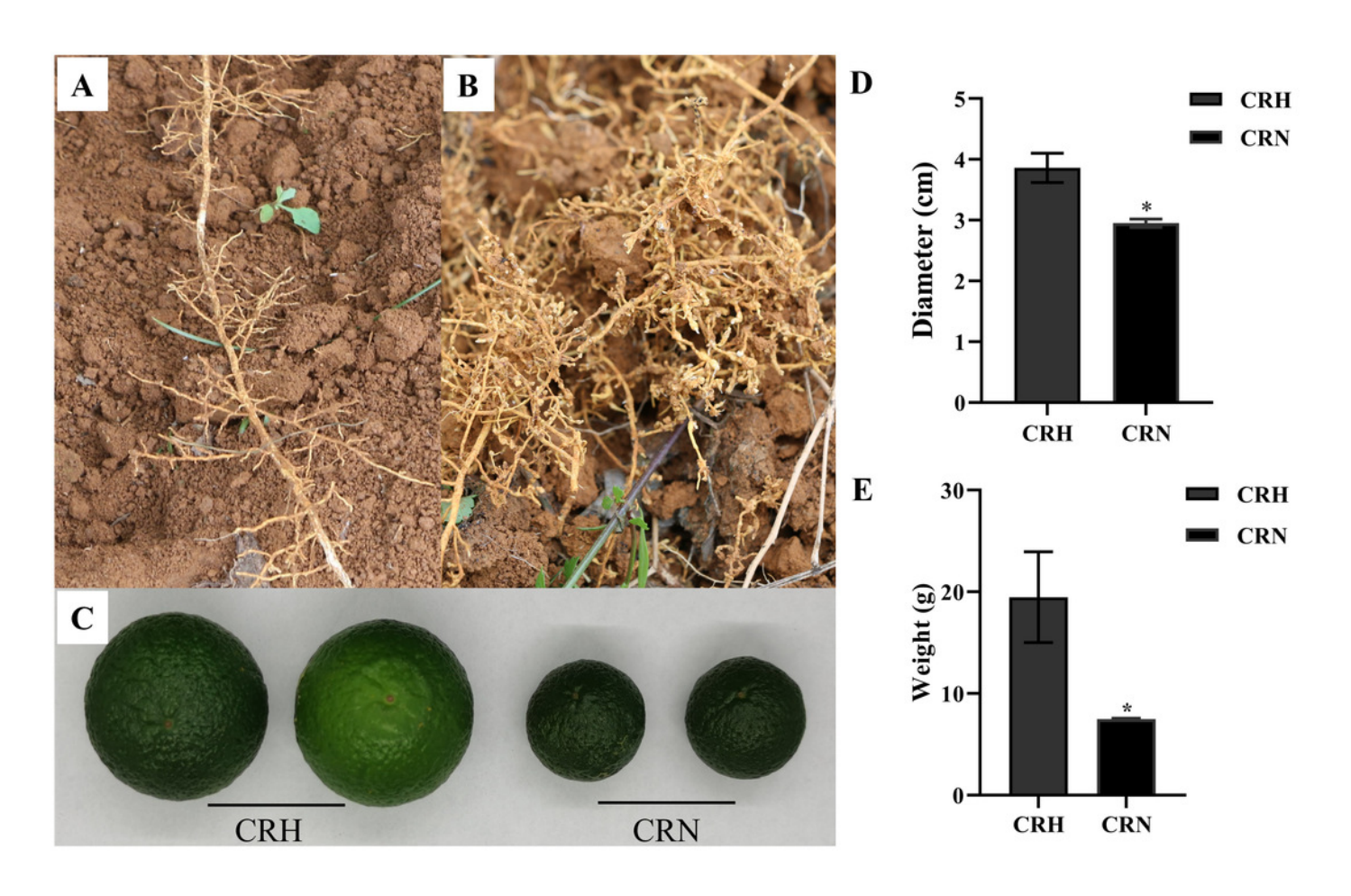


- 674 biotechnological approaches. Journal of the American Society for Horticultural Science American Society for
- 675 *Horticultural Science* 133(1): 177-126.
- 676 Vrain TC. 1993. Restriction Fragment Length Polymorphism Separates Species of the Xiphinema americanum
- 677 Group. *Journal of Nematology* 25(3): 361-4.
- Wang C, Henkes LM, Doughty LB, He M, Wang D, Meyer-Almes FJ, Cheng YQ. 2011. Thailandepsins:
- 679 bacterial products with potent histone deacetylase inhibitory activities and broad-spectrum antiproliferative
- 680 activities. Natural Products Journal 74(10): 2031-8.
- Wang R, Wang T, Li EF. 2021. Research advances of biocontrol Bacillus in the field of plant diseases (in
- 682 Chinese with English abstract). *Journal of Tianjin Agricultural University* 28(04): 71-77.
- Wang R, Zhang H, Sun L, Qi G, Chen S, Zhao X. 2017. Microbial community composition is related to soil
- 684 biological and chemical properties and bacterial wilt outbreak. Scientific Reports 7(1): 343.
- 685 Wang XL, Li JH, Peng DL. 2007. Cloning and sequence analysis of rDNA-ITS fragment of root-knot
- 686 mematodes (in Chinese with English abstract). *Journal of Huazhong Agricultural University* 05: 624-628.
- 687 Wolfgang A, Taffner J, Guimares RA, Coyne D, Berg G. 2019. Novel strategies for soil-borne diseases:
- 688 exploiting the microbiome and volatile-based mechanisms toward controlling meloidogyne-based disease
- 689 complexes. Frontiers in Microbiology 7(10): 1296.
- 690 Xian HQ, Tang W, Zhang LQ, Li AN, Li DC. 2012. Cloning and expression of a chitinase gene tfchi1 from
- 691 Talaromyces flavus and the antifungal activity of the recombinant enzyme. Acta Phytopathologica Sinica
- 692 42(02): 146-153.
- 693 Yang Y, Hu X, Liu P, Chen L, Peng H, Wang Q, Zhang Q. 2021. A new root-knot nematode, *Meloidogyne*
- 694 vitis sp. nov. (Nematoda: Meloidogynidae), parasitizing grape in Yunnan. Plos One 16(2): e0245201.
- 695 Zhang FR. 2020. Rhizosphere microorganisms: the second genome of plants that play an important role in the
- 696 green development of agriculture. *Biotechnology Bulletin* 36(09): 1-2.
- 697 Zhang Y, Hu A, Zhou J, Zhang W, Li P. 2020. Comparison of bacterial communities in soil samples with and
- 698 without tomato bacterial wilt caused by *Ralstonia solanacearum* species complex. *BMC Microbiology* 20(1):
- 699 89.

Damage symptom of root-knot nematodes on Orah and its effect on yield.

Figure 1. Damage symptom of root-knot nematodes on Orah and its effect on yield.

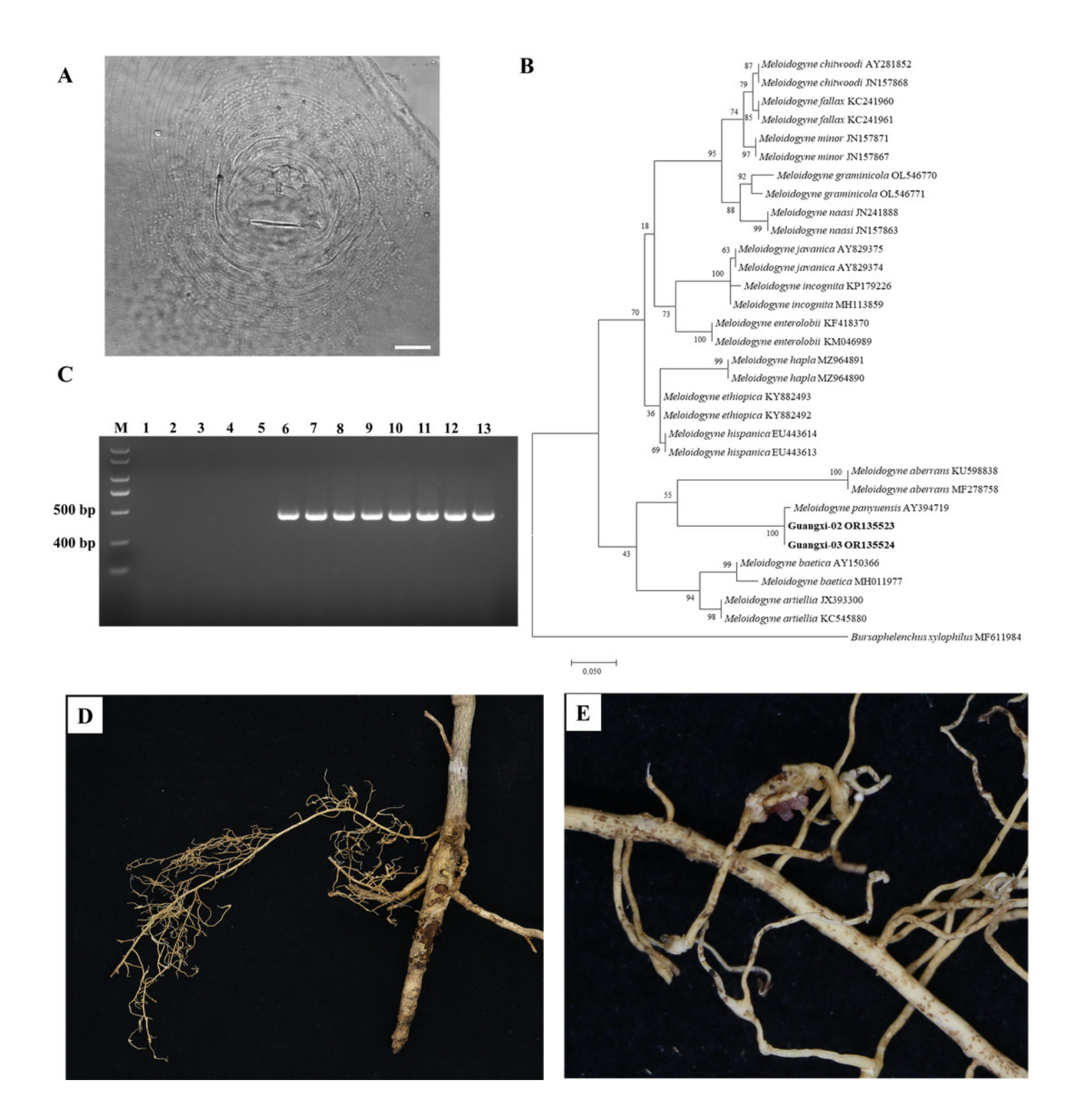
A, roots of healthy Orah. B, roots of root-knot nematodes infected Orah. C, the fruit appearance of the healthy Orah (CRH) and the root-knot nematodes infected Orah (CRN). D, the diameter of fruits. E, the mass of fruits.





Identification of rot-knot nematode infecting Orah.

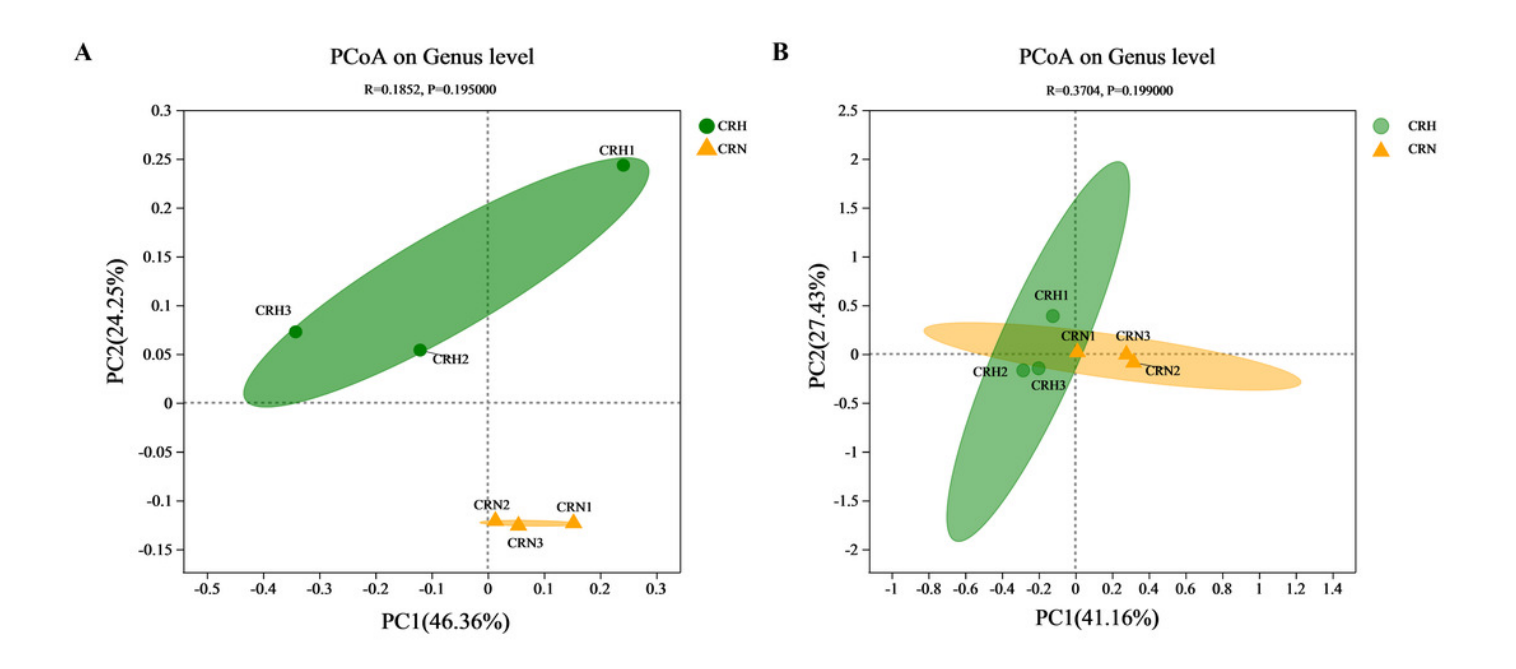
Figure 2. Identification of rot-knot nematode infecting Orah. A, Perineal pattern of nematode female isolated from infected Orah root. Scale bar: 20 μm. B, phylogenetic tree based on rDNA-ITS of *Meloidogyne* spp.. C, specific amplification using the primers Mp-F/Mp-R in *M. panyuensis* isolated from infected Orah. M: DL 2000 Plus; 1-5: negative control (1. Water; 2-3. *M. incognita*; 4-5. *M. enterolobii*.); 6-13: *M. panyuensis*. D-E, the disease symptoms on Orah caused by *M. panyuensis*.





Principal coordinate analysis (PCoA) of bacterial (A) and fungal (B) communities based on bray-curtis distances.

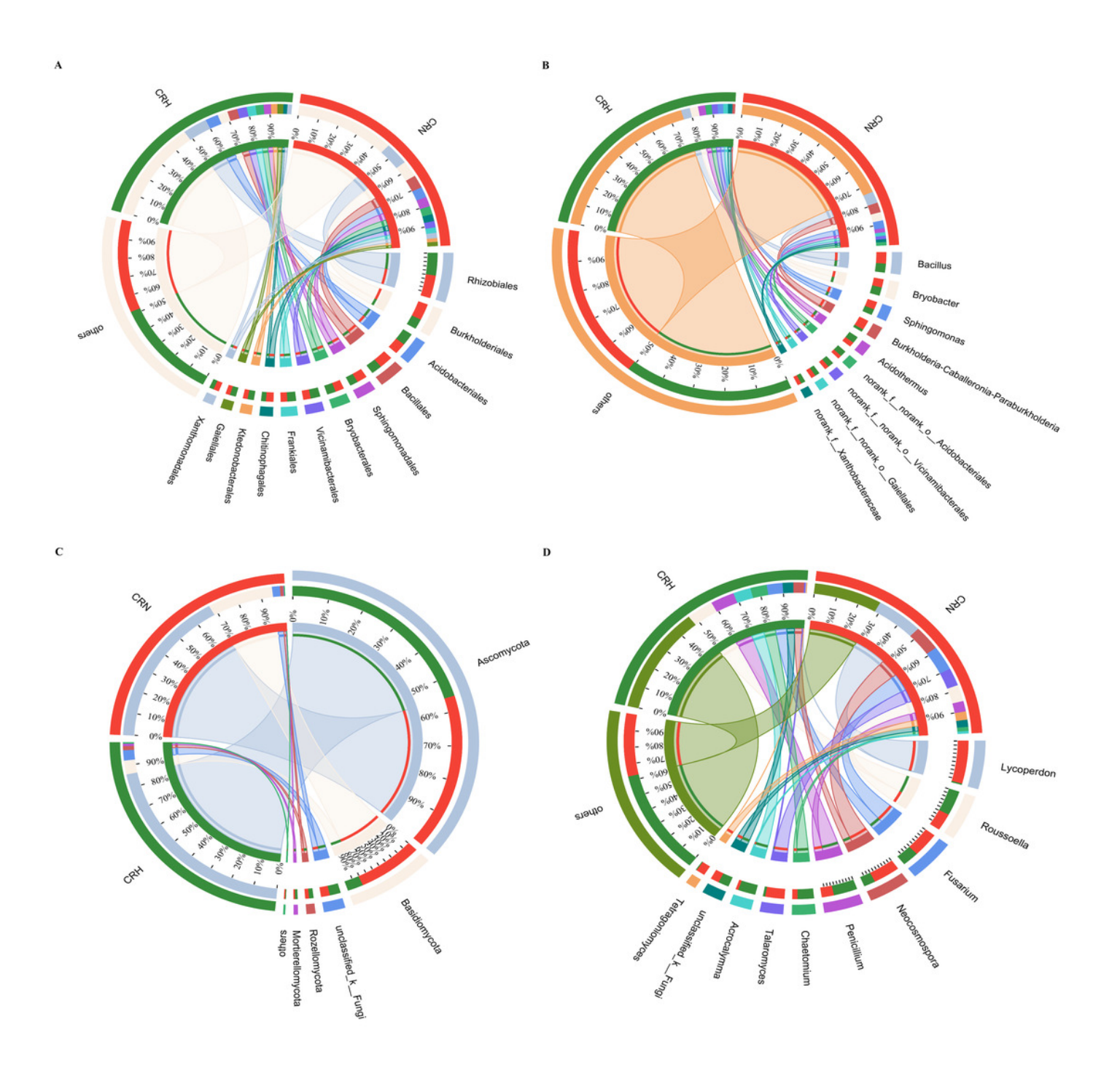
Figure 3. Principal coordinate analysis (PCoA) of bacterial (A) and fungal (B) communities based on bray-curtis distances.





Relationship between species and samples in rhizosphere soil of healthy and *M. panyuensis*-infected.

Figure 4. Relationship between species and samples in rhizosphere soil of healthy and *M. panyuensis*-infected. A (order level) and B (genus level) were the bacterial community; C (phylum level) and D (genus level) were the bacterial community.



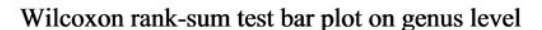


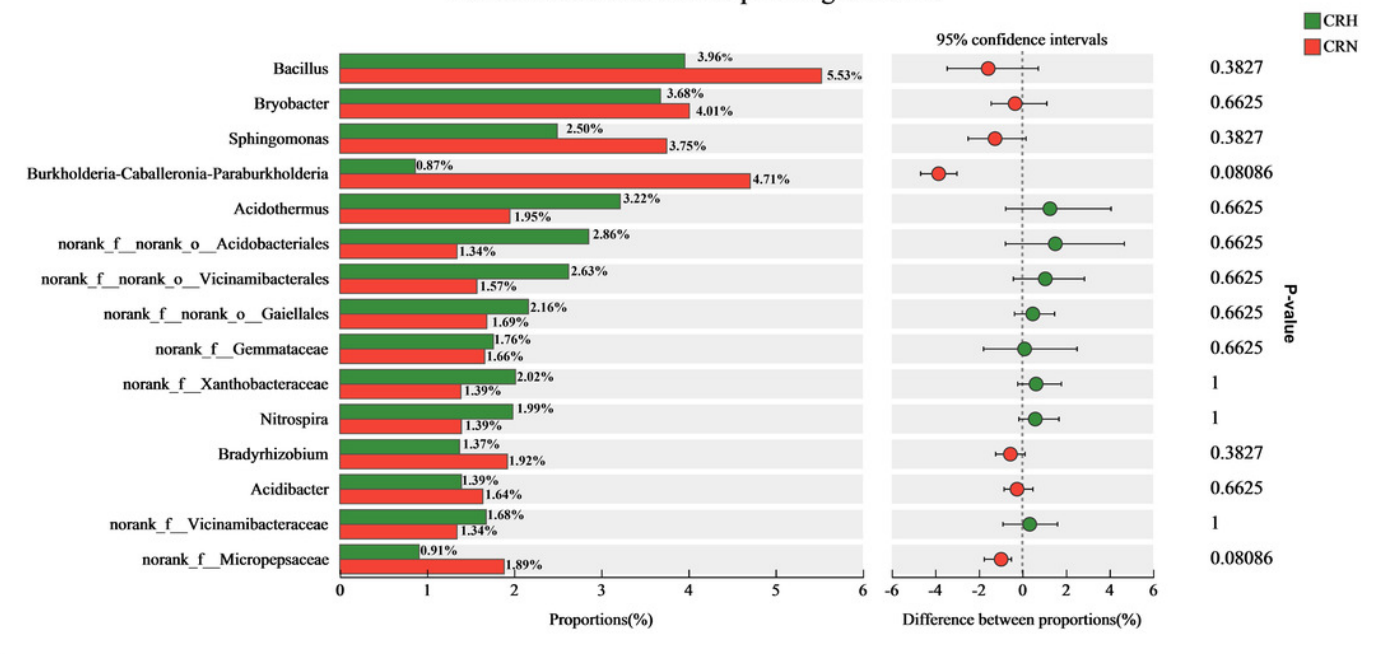
Comparative analysis of bacterial (A) and fungal (B) community in rhizosphere soil of healthy and *M. panyuensis*-infected.

Figure 5. Comparative analysis of bacterial (A) and fungal (B) community in rhizosphere soil of healthy and *M. panyuensis*-infected.

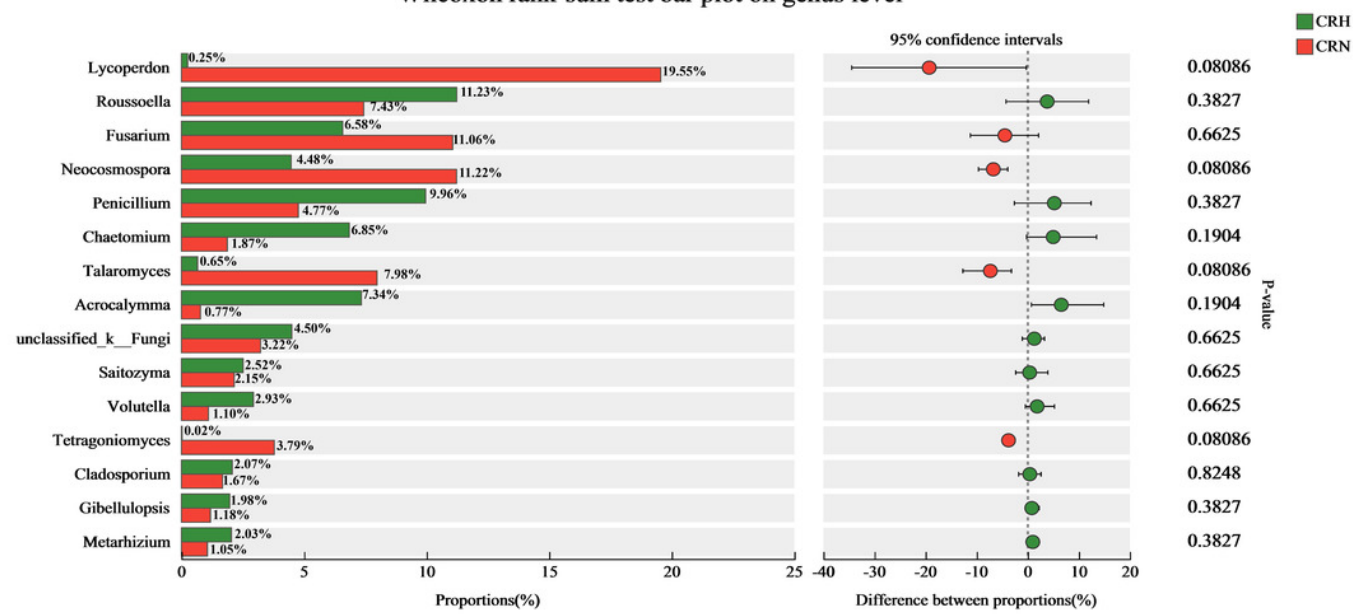


В





Wilcoxon rank-sum test bar plot on genus level





Redudancy analysis (RDA) between healthy and *M. panyuensis*-infected Orah rhizosphere soil microbial communities and environmental factors

Figure 6. Redudancy analysis (RDA) between healthy and *M. panyuensis*-infected Orah rhizosphere soil microbial communities and environmental factors. A and B were the bacterial community; C and D were the fungal community.

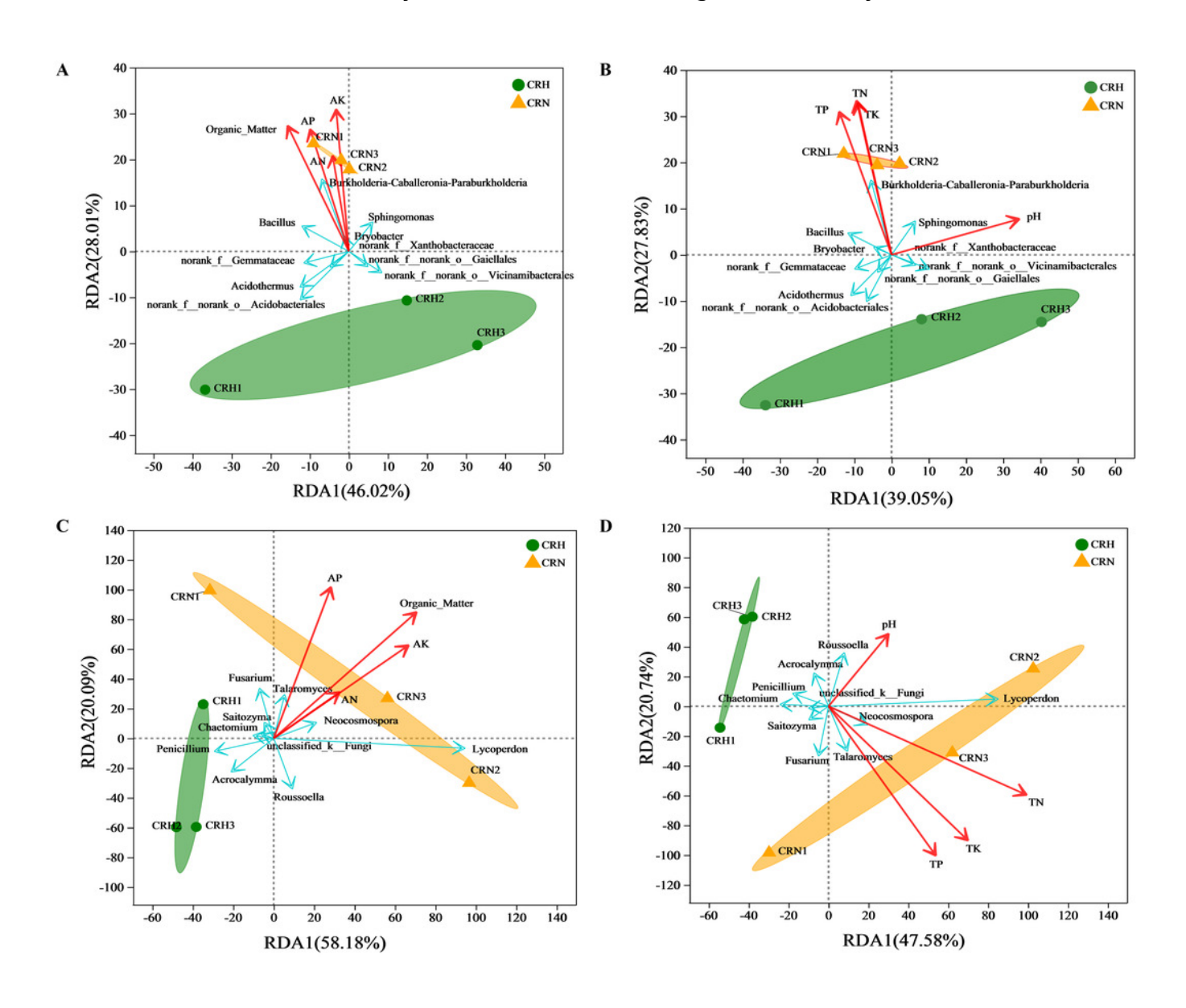




Table 1(on next page)

Soil chemical properties of the healthy and *M. panyuensis*-infected Orah rhizosphere soil.

Table 1. Soil chemical properties of the healthy and *M. panyuensis*-infected Orah rhizosphere soil.



Table 1. Soil chemical properties of the healthy and *M. panyuensis*-infected Orah rhizosphere soil.

Number	Samples	рН	Organic matter (g/kg)	AN (mg/kg)	AP (mg/kg)	AK (mg/kg)	TN (g/kg)	TP (g/kg)	TK (g/kg)
1	CRH	5.02±0.94 a	23.10±4.70 a	123.95±25.55 a	44.56±28.04 a	215.42±68.84 a	1.40±0.13 a	1.30±0.07 a	2.34±0.04 a
2	CRN	5.06±0.20 a	36.70±1.21 b	141.79±3.66 a	276.89±128.40 b	430.40±26.75 b	1.92±0.06 b	1.98±0.25 b	3.05±0.20 b



Table 2(on next page)

Richness and diversity estimation of the 16S and ITS1 sequencing libraries in healthy and *M. panyuensis*-infected Orah rhizosphere soil.

Table 2. Richness and diversity estimation of the 16S and ITS1 sequencing libraries in healthy and *M. panyuensis*-infected Orah rhizosphere soil.

Table 2. Richness and diversity estimation of the 16S and ITS1 sequencing libraries in healthy and *M. panyuensis*-infected Orah rhizosphere soil.

Category	Group	Coverage	Chao 1	Simpson	Shannon
Bacteria	CRH	0.9996	840±77 a	0.003±0.0003 a	6.26±0.07 a
Dacteria	CRN	0.9992	937±133 a	0.0025±0.0003 a	6.39±0.14 a
Eunai	CRH	1	370±75 a	0.0469±0.0093 a	3.98±0.1 a
Fungi	CRN	1	262±35 a	0.0761±0.02 a	3.5±0.29 a